Supporting Information

Interfacial Microenvironment Regulation of FeOOH/S-Co Heterostructure Catalyst via S Atoms for Overall Water Splitting

Zehao Zang[†], Yangyang Ren[†], Xiang Li[‡], Yahui Cheng[§], Lanlan Li[†], Xiaofei Yu[†], Xiaojing Yang[†], Zunming Lu[†], Xinghua Zhang[†,*], Hui Liu[//,*]

[†]School of Materials Science and Engineering, Hebei University of Technology, Tianjin 300130, China

[‡]Graduate School, Hebei University of Technology, Tianjin 300401, China

[§]Tianjin Key Laboratory of Process Control and Green Technology for Pharmaceutical Industry, Department of Electronics, Nankai University, Tianjin 300350, China

[//]School of Materials Science and Engineering, Tianjin University, Tianjin 300072, China.

* Corresponding author, Email: zhangxinghua@hebut.edu.cn; hui_liu@tju.edu.cn.

Experimental Sections

Preparation of the Co/NF. The Co/NF catalyst was synthesized through a typical electrodeposition method in a two-electrode cell on a digital control DC power supply. Nickel foam (NF, 2 × 3 cm^2) and carbon paper (CP, 2 × 3 cm^2) were served as cathode and anode, respectively. All the electrodeposition was performed at room temperature and the distance between cathode and anode electrodes was maintained at 3 cm. The NF was washed by 3.0 M HCl, water and ethanol, and the CP was also washed by water and ethanol. To obtain Co/NF, 50 mM $CoCl_2 \cdot 6H_2O$ and 1.25 M NH_4F were added into 50 mL deionized water to form electrolytes. After different deposition potential attempts, the electrodeposition process was finally conducted at 3.5 V for 0.5 h at room temperature. Then the sample was washed and dried in the air. The loading of Co/NF catalyst is 13.3 mg cm^{-2}.

Preparation of the FeOOH/NF. The FeOOH/NF catalyst was also synthesized via electrodeposition. However, this process was carried out on CHI750E using NF (2 × 3 cm^2), CP (2 × 3 cm^2) and saturated calomel electrode (SCE) as working, counter and reference electrodes. The electrodeposition was performed in an aqueous solution with 10 mM $Fe(NO_3)_3 \cdot 9H_2O$ and 0.89 g alanine at room temperature with −1.2 V for 600 s. The loading of FeOOH/NF catalyst is 2.0 mg cm^{-2}.

Preparation of the FeOOH/Co/NF and FeOOH/S-Co/NF. To obtain the FeOOH/Co/NF, the Co/NF was immersed into 15 mL solution with 100 mM $FeSO_4 \cdot 9H_2O$ for 15 min at room temperature and the adsorbed Fe^{2+} ions were oxidized to FeOOH during this process, then washed and dried in the air. The loading

of FeOOH/Co/NF is 15.7 mg cm^{-2}. The FeOOH/S-Co/NF catalyst was obtained with the similar process and the only difference is that 1 M thiourea (TU) was added into the electrolyte when preparing the Co/NF, which is named S-Co/NF. The loading of FeOOH/S-Co/NF catalyst is 18.5 mg cm^{-2}. During this process, the possible reactions are as follows. First, Co^{2+} or the complex ions of $Co(TU)_2^{2+}$ was reduced into metallic Co at 3.5 V. The dissociative TU can adsorb on the generated metallic Co and subsequently be reduced at 3.5 V to form S-Co. When S-Co was immersed into $FeSO_4$ solution, the adsorbed Fe^{2+} was oxidized by the dissolved oxygen in the solution to form FeOOH/S-Co.

Additionally, the FeOOH/S-Co catalyst was also prepared on carbon paper (FeOOH/S-Co/CP) in the same conditions with FeOOH/S-Co/NF. The loading of FeOOH/S-Co/CP is 18.2 mg cm^{-2}, which is similar to that of FeOOH/S-Co/NF.

Preparation of the Pt/C/NF and RuO_2/C/NF. Electrode ink was obtained by adding 20% Pt/C (5 mg) into 720 μL deionized water, 250 μL isopropanol and 30 μL Nafion for 30 min after ultrasonic dispersion. The RuO_2 electrode ink was prepared in the same method, except that 5 mg Pt/C was replaced with 2 mg RuO_2 and 3 mg carbon black. 50 μL ink was dropped on NF (1 cm × 1 cm) to serve as Pt/C/NF or RuO_2/C/NF.

Characterizations. The structure and morphology of all the samples were performed through scanning electron microscopy (SEM, JSM-7100F) and transmission electron microscopy (TEM, FEI Tecnai G2 F20). The X-ray power diffraction patterns (XRD) of FeOOH/S-Co, FeOOH/Co, FeOOH and Co catalysts

were performed on Bruker D8 Discover and their X-ray photoelectron spectroscopy (XPS) were collected on ESCALAB 250Xi. The Raman spectra of FeOOH/S-Co and FeOOH/Co samples were carried out on LabRAM HR Evolution at 532 nm excitation.

The electrochemical in-situ Raman measurements were also obtained on LabRAM HR Evolution with an excitation source of 532 nm. A specially designed cell was used for in-situ Raman tests, in which Pt wire, Ag/AgCl electrode and FeOOH/S-Co/NF (1 cm × 1 cm) serve as counter electrode, reference electrode and working electrode, respectively. The Raman spectra were recording after applying various potentials for 3 min.

Electrochemical measurements. Electrochemical measurements were conducted using CHI750E in a three-electrode system containing working electrode (NF loaded with prepared catalysts), reference electrode (saturated calomel electrode, SCE) and counter electrode (graphite rod). All potentials were converted to reversible hydrogen electrode (RHE): $E_{RHE} = E_{SCE} + 0.244 + 0.059 \times pH$. Linear sweep voltammetry (LSV) was recorded at a scan rate of 5 mV s^{-1} with 95% iR compensation, unless otherwise stated. To eliminate the influence of oxidation peak of NF, the LSV curves of all catalysts for OER were obtained via a negative scan. Electrochemical impedance spectroscopy (EIS) was carried out at frequency between 1000 kHz and 0.1 Hz. The double layer capacitance (C_{dl}) was estimated via cyclic voltammetry (CV) at scan rates from 5 to 30 mV s^{-1} in a non-Faradaic potential window. The Faradaic efficiency (FE) was calculated by the formula: $FE = \frac{V_a}{V_t} \times 100\%$ (V_a: actual measured

gas volumes; V_t: theoretical gas volumes.) and $V_t = (I \times t)/(n \times F) \times V_m$ (I: current, mA; t: time, s; n: transferred electron number; F: Faradaic constant, 96485 C mol^{-1}; V_m: gas molar volume, 22.4 L mol^{-1}). In addition, the turnover frequency (TOF) was calculated according to the equation: $TOF = (j \times S)/(n \times F \times N)$, in which all metal atoms were considered as the active sites. (j: current density, mA cm^{-2}; S: geometric area of electrode, cm^{-2}; n: transferred electron number; F: Faradaic constant, 96485 C mol^{-1}; N: the number of active sites, mol).

Computational Methods. The spin-polarized density function theory (DFT) calculations were performed via the Vienna Ab-initio Simulation Package (VASP) with plane wave basis sets and projector-augmented wave (PAW) pseudopotentials.[1-3] The generalized gradient approximation (GGA) developed by Perdew−Burke−Ernzerhof (PBE) was adopted for the exchange-correlation functionals.[4] The converged cutoff energy for plane-wave basis set was 450 eV and the k-point mesh for Brillouin zone was set to be 3 × 3 × 1. The convergence criterion for geometry optimization was set to be 1 × 10^{-5} eV for energy change and 0.05 eV/Å for structural optimization.

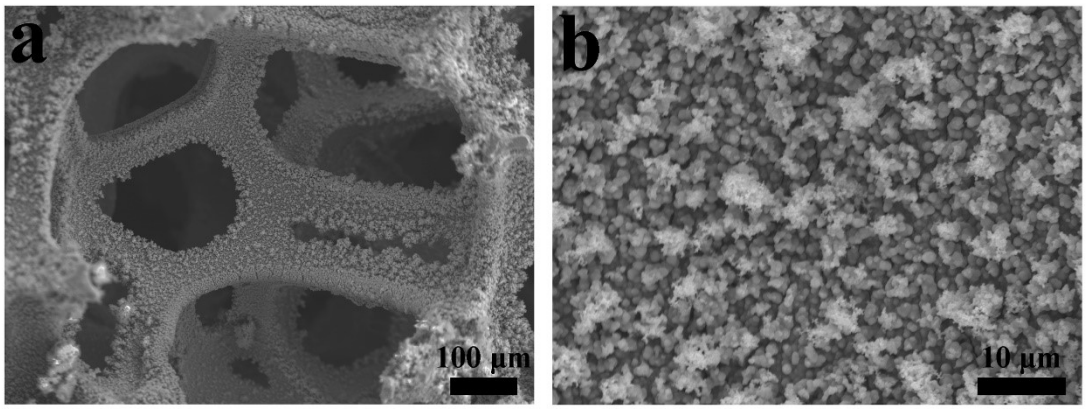

Fig. S1 The SEM images of S-Co/NF catalyst at (a) low magnification, and (b) high magnification.

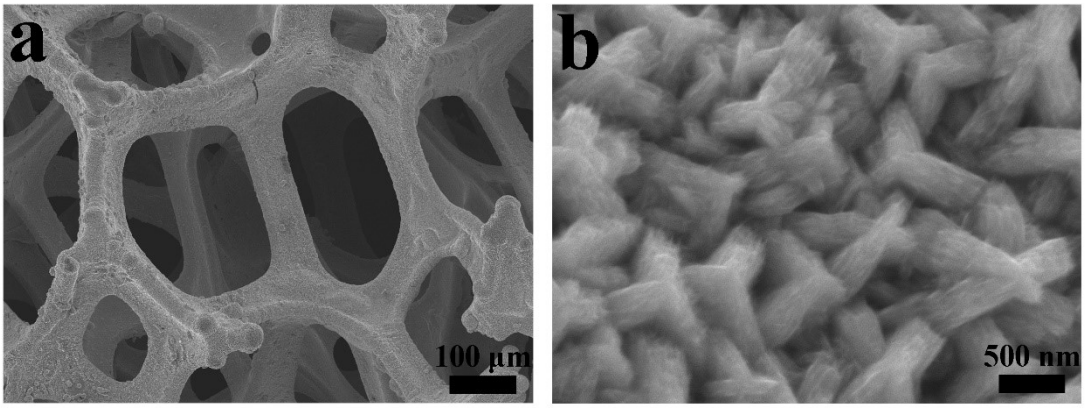

Fig. S2 The SEM images of Co/NF sample at (a) low magnification, and (b) high magnification.

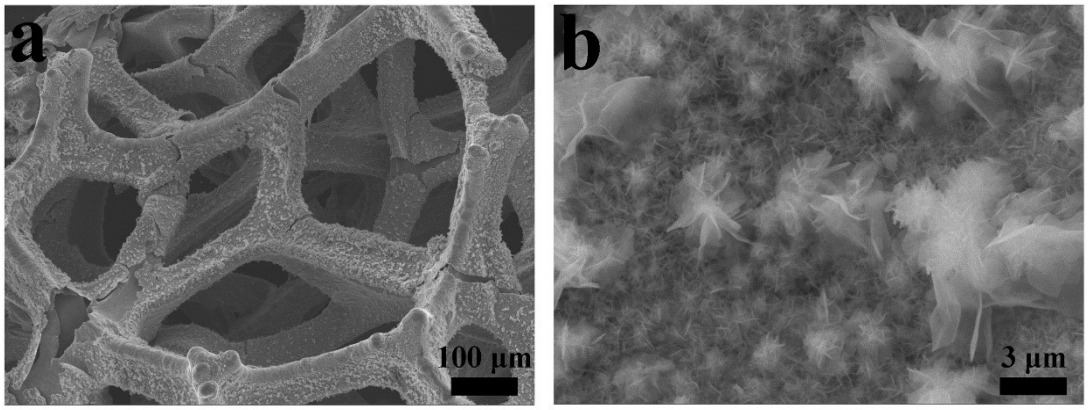

Fig. S3 The SEM images of FeOOH/Co/NF catalyst at (a) low magnification, and (b) high magnification.

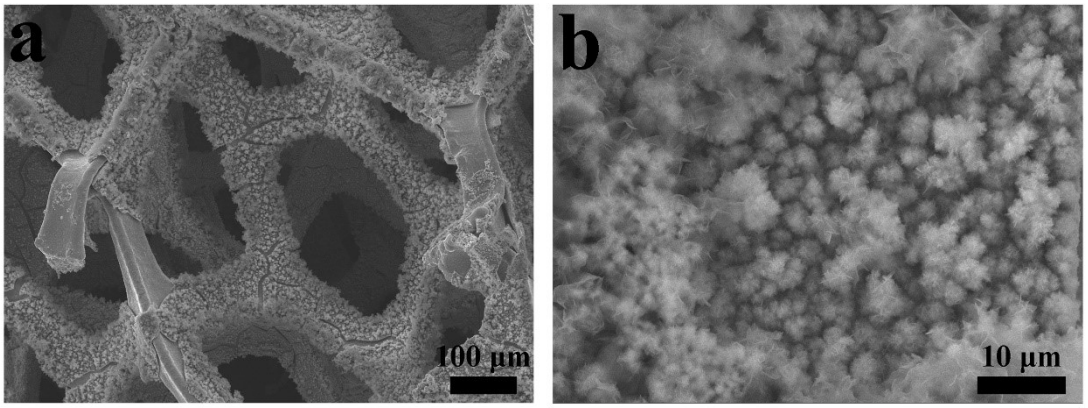

Fig. S4 The SEM images of FeOOH/S-Co/NF catalyst at (a) low magnification, and (b) high magnification.

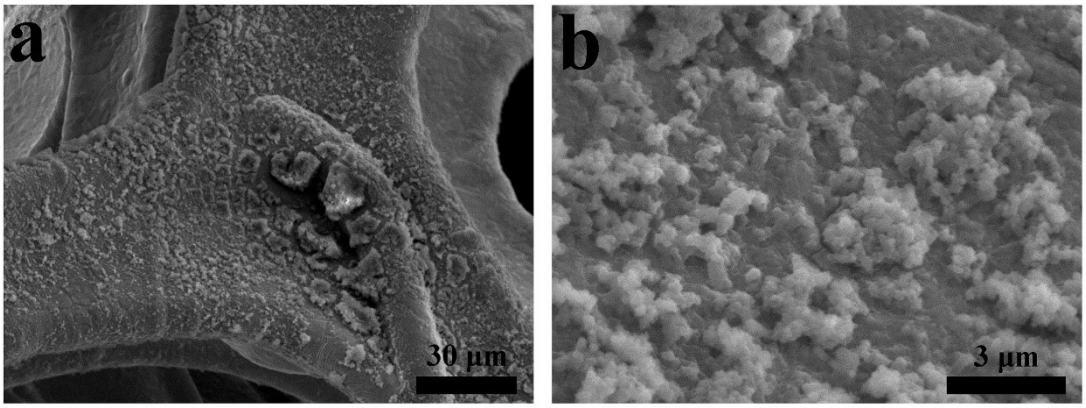

Fig. S5 The SEM images of FeOOH/NF catalyst at (a) low magnification, and (b) high magnification.

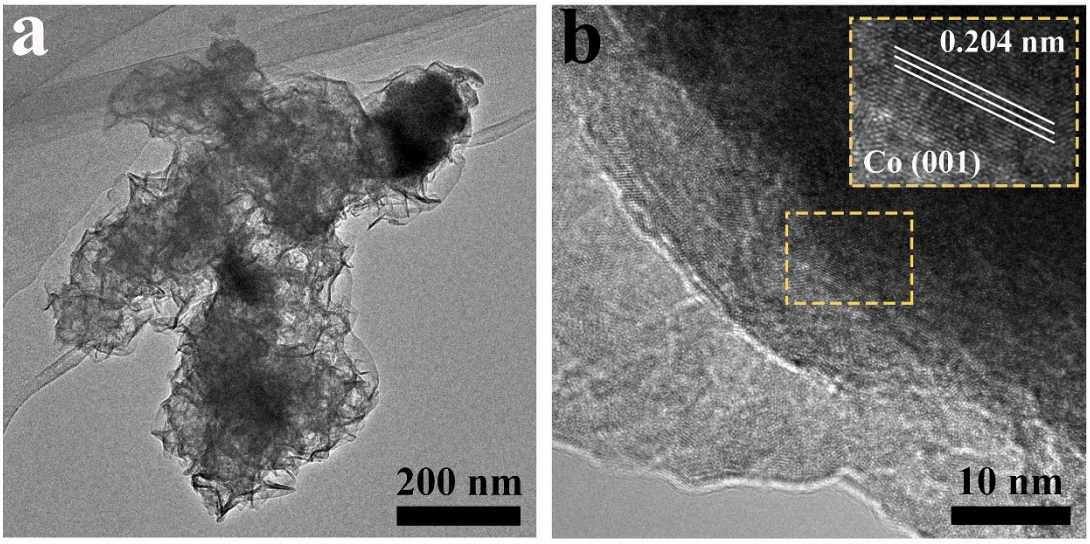

Fig. S6 (a) TEM image, and (b) HRTEM image of Co sample.

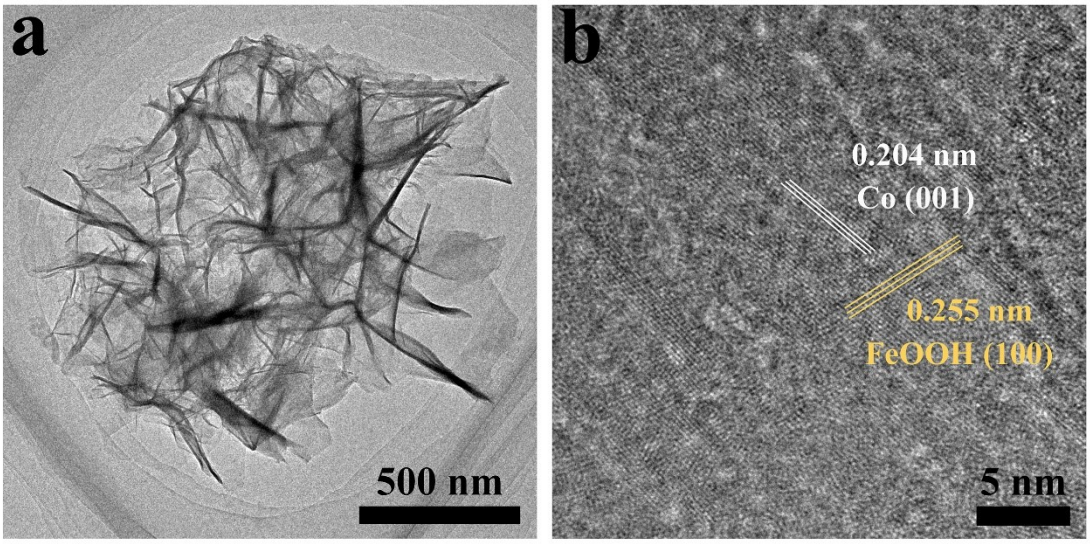

Fig. S7 (a) TEM image, and (b) HRTEM image of FeOOH/Co catalyst.

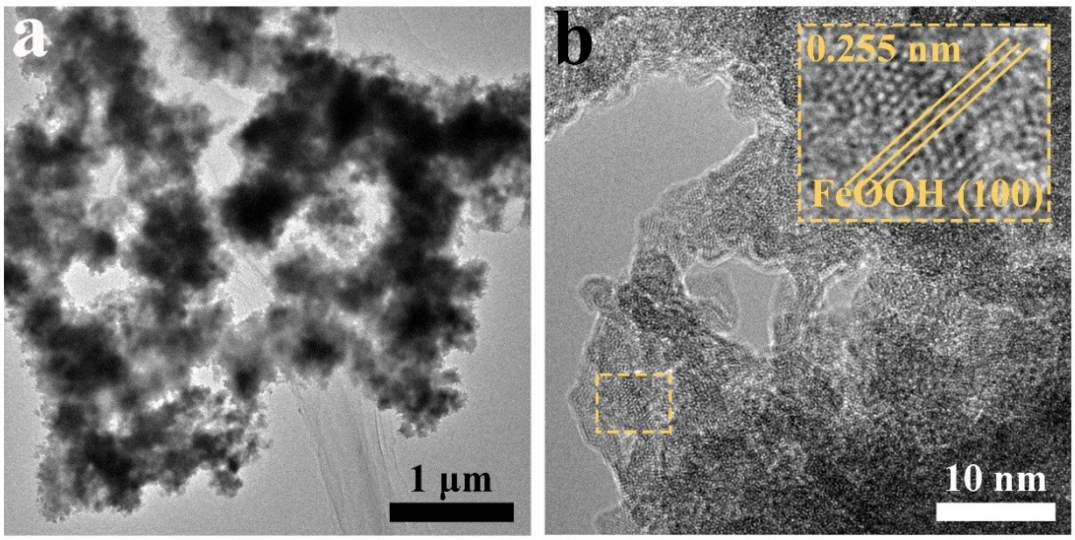

Fig. S8 (a) TEM image, and (b) HRTEM image of FeOOH catalyst.

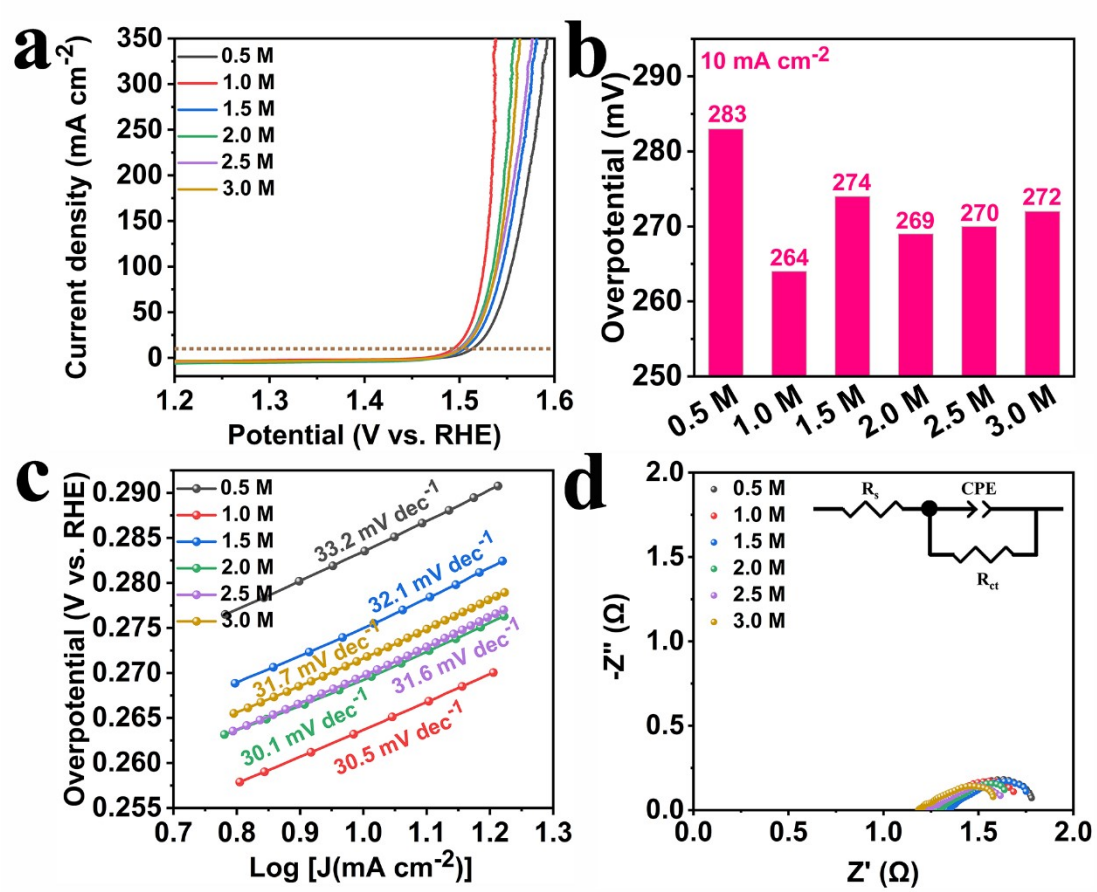

Fig. S9 The OER performance in 1.0 M KOH for FeOOH/S-Co catalysts prepared with different thiourea concentrations. (a) Polarization curves with a scan rate of 5 mV s^{-1}, (b) corresponding comparison of overpotentials at 10 mA cm^{-2}, (c) Tafel plots, (d) EIS curves.

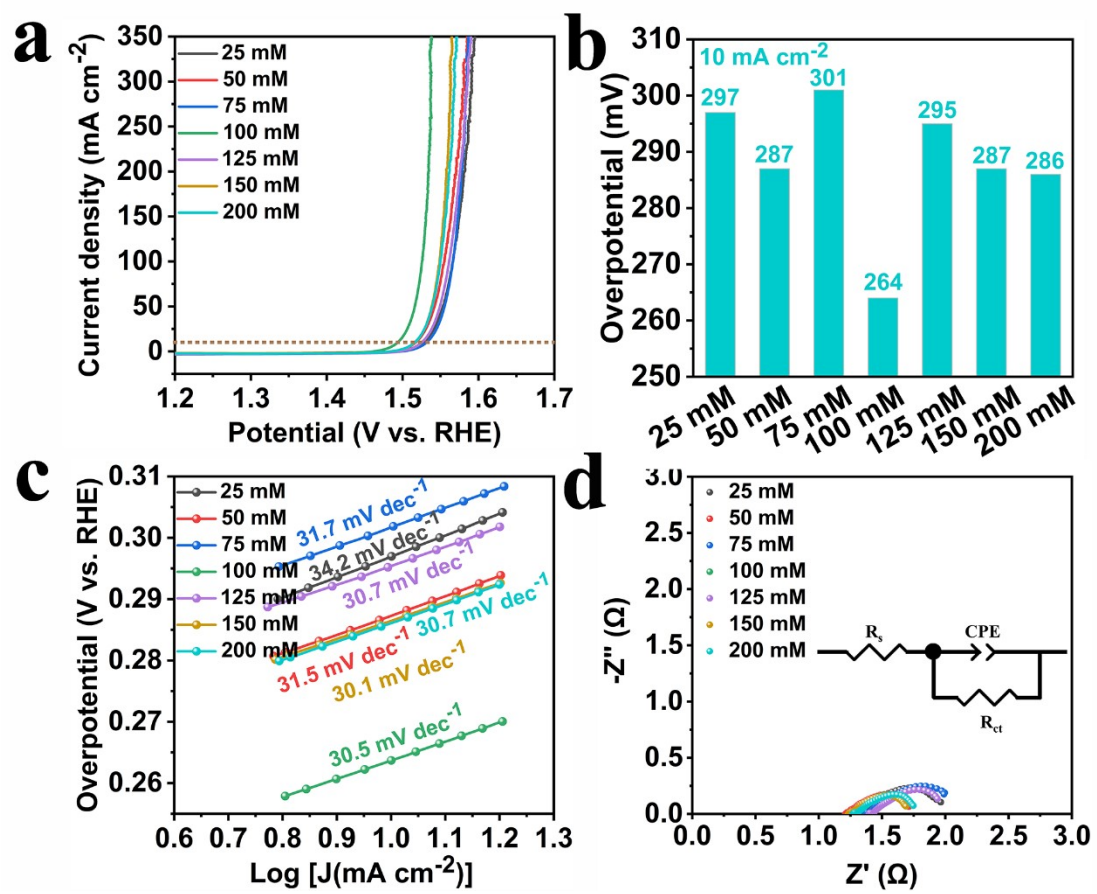

Fig. S10 The OER performance in 1.0 M KOH for FeOOH/S-Co catalysts prepared with different $FeSO_4$ concentrations. (a) Polarization curves with a scan rate of 5 mV s^{-1}, (b) corresponding comparison of overpotentials at 10 mA cm^{-2}, (c) Tafel plots, (d) EIS curves.

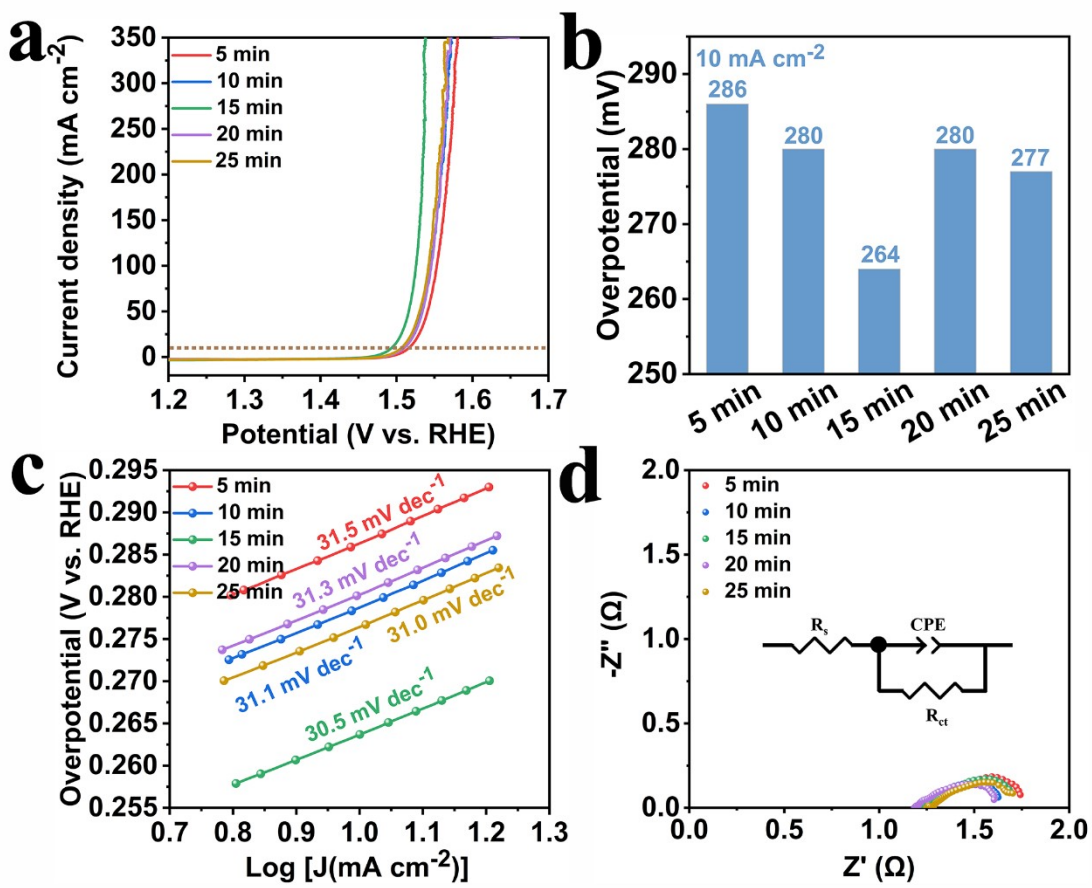

Fig. S11 The OER performance in 1.0 M KOH for FeOOH/S-Co catalysts prepared with different soaking time in $FeSO_4$. (a) Polarization curves with a scan rate of 5 mV s^{-1}, (b) corresponding comparison of overpotentials at 10 mA cm^{-2}, (c) Tafel plots, (d) EIS curves.

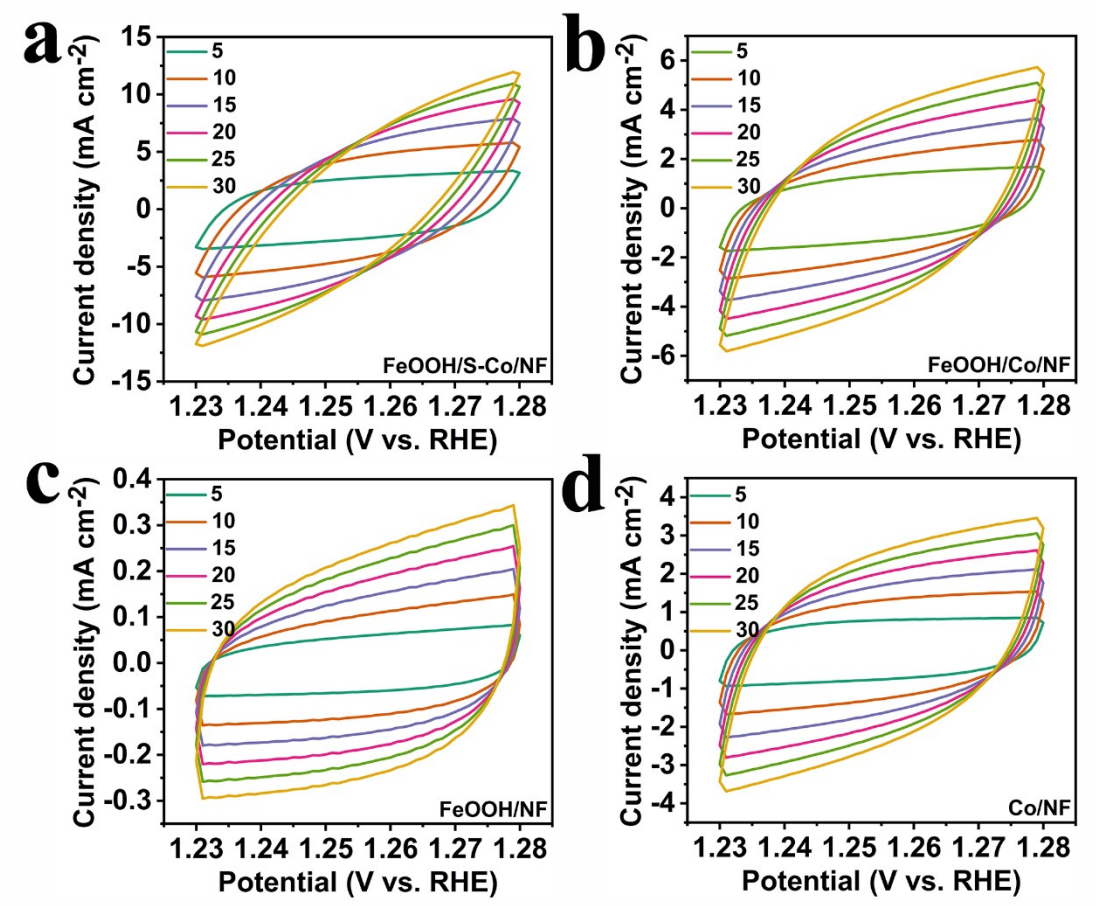

Fig. S12 CV curves of (a) FeOOH/S-Co/NF, (b) FeOOH/Co/NF, (c) FeOOH/NF and (d) Co/NF catalyst recorded in O_2 saturated 1.0 M KOH solution with different scan rates.

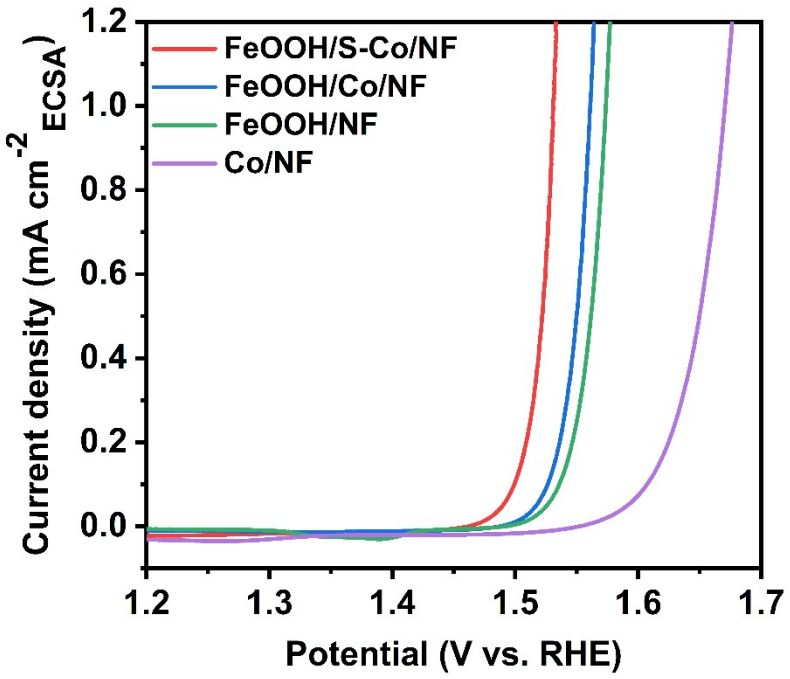

Fig. S13 The OER polarization curves normalized by ECSA for FeOOH/S-Co/NF, FeOOH/Co/NF, FeOOH/NF and Co/NF catalysts.

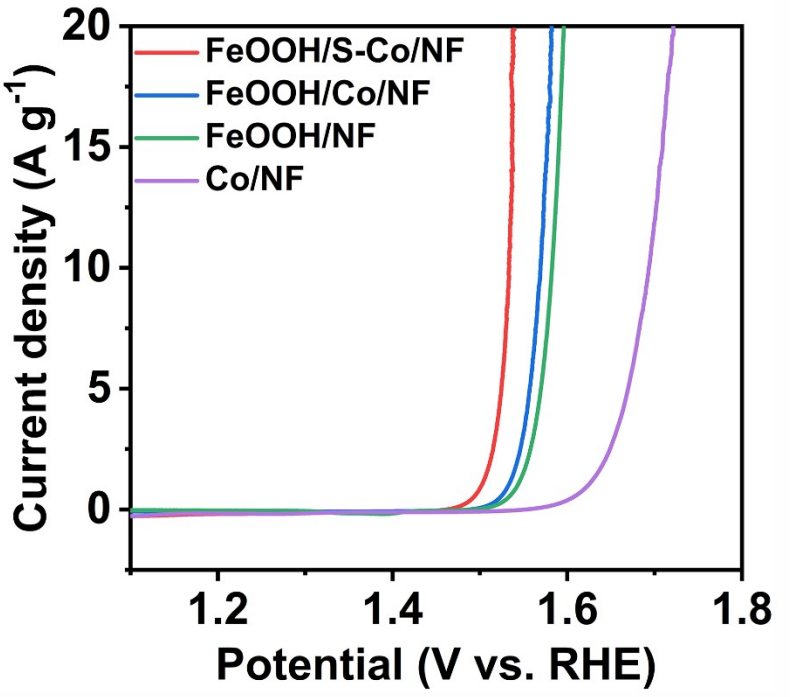

Fig. S14 The OER polarization curves normalized by mass for FeOOH/S-Co/NF, FeOOH/Co/NF, FeOOH/NF and Co/NF catalysts.

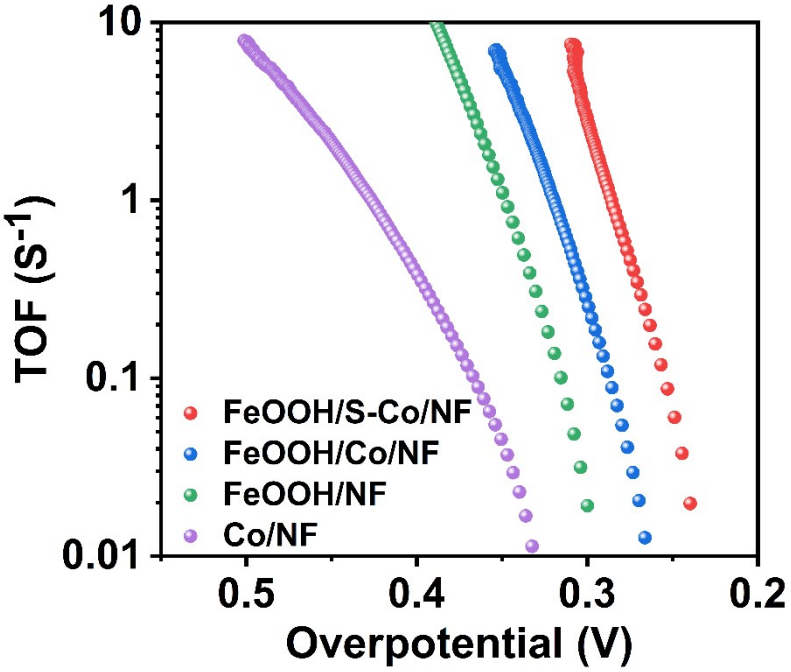

Fig. S15 The TOF values of FeOOH/S-Co/NF, FeOOH/Co/NF, FeOOH/NF and Co/NF catalysts for OER.

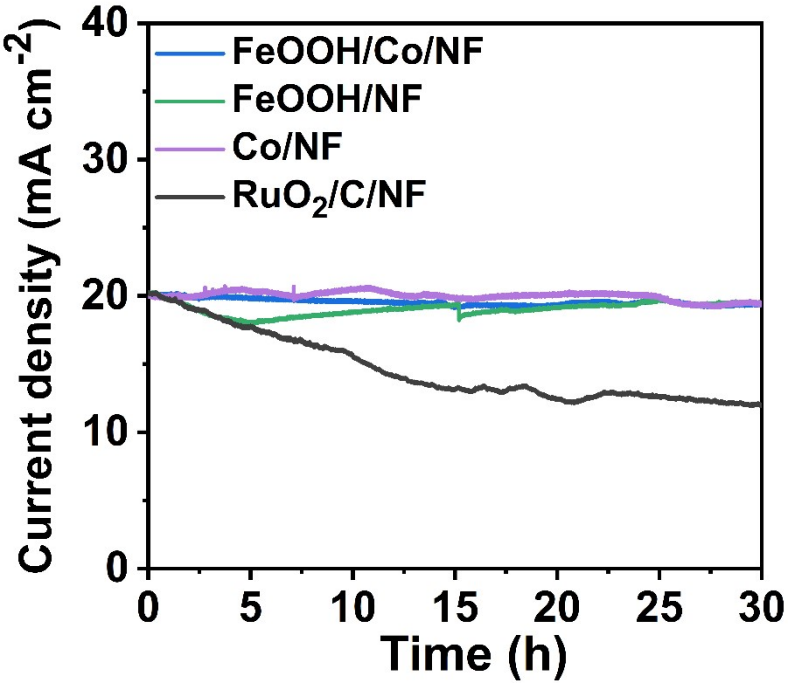

Fig. S16 I-t curves of FeOOH/Co/NF, FeOOH/NF, Co/NF and RuO_2/C/NF catalysts at 1.567 V, 1.606 V, 1.666 V and 1.660 V for 30 h.

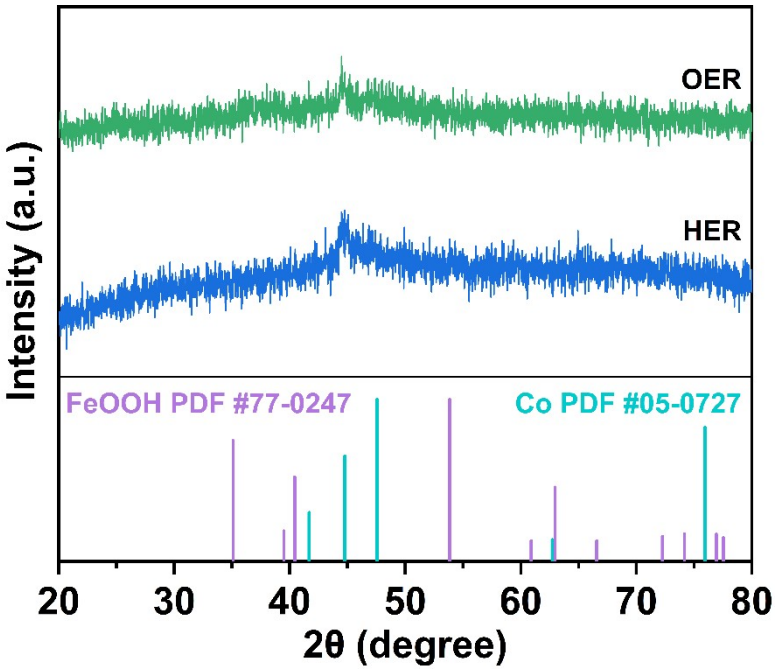

Fig. S17 XRD patterns of the FeOOH/S-Co/NF catalyst after HER and OER i-t test at 20 mA cm^{-2} for 30 h.

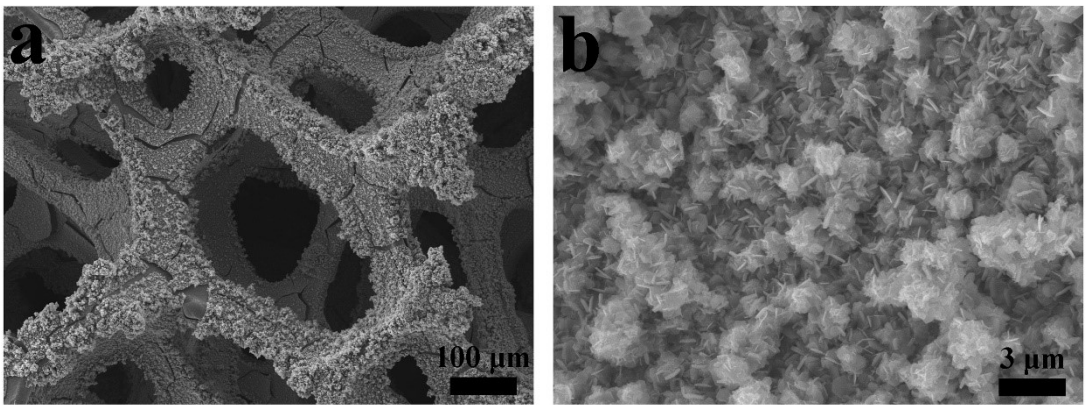

Fig. S18 The SEM images of FeOOH/S-Co/NF catalyst after OER i-t test at 20 mA cm^{-2} for 30 h.

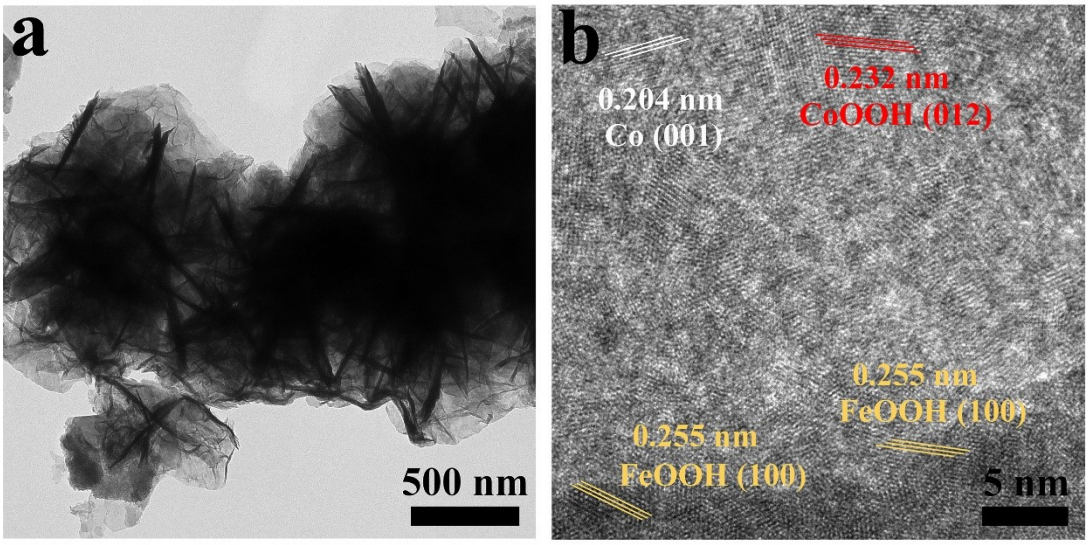

Fig. S19 (a) TEM and (b) HRTEM images of FeOOH/S-Co/NF catalyst after OER i-t test at 20 mA cm^{-2} for 30 h.

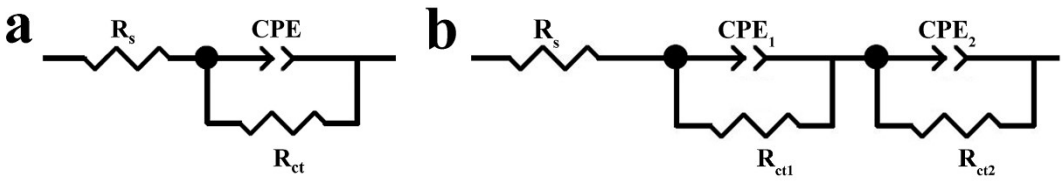

Fig. S20 Equivalent circuit of (a) FeOOH/S-Co/NF, FeOOH/NF, Co/NF catalysts, and (b) Pt/C/NF for HER.

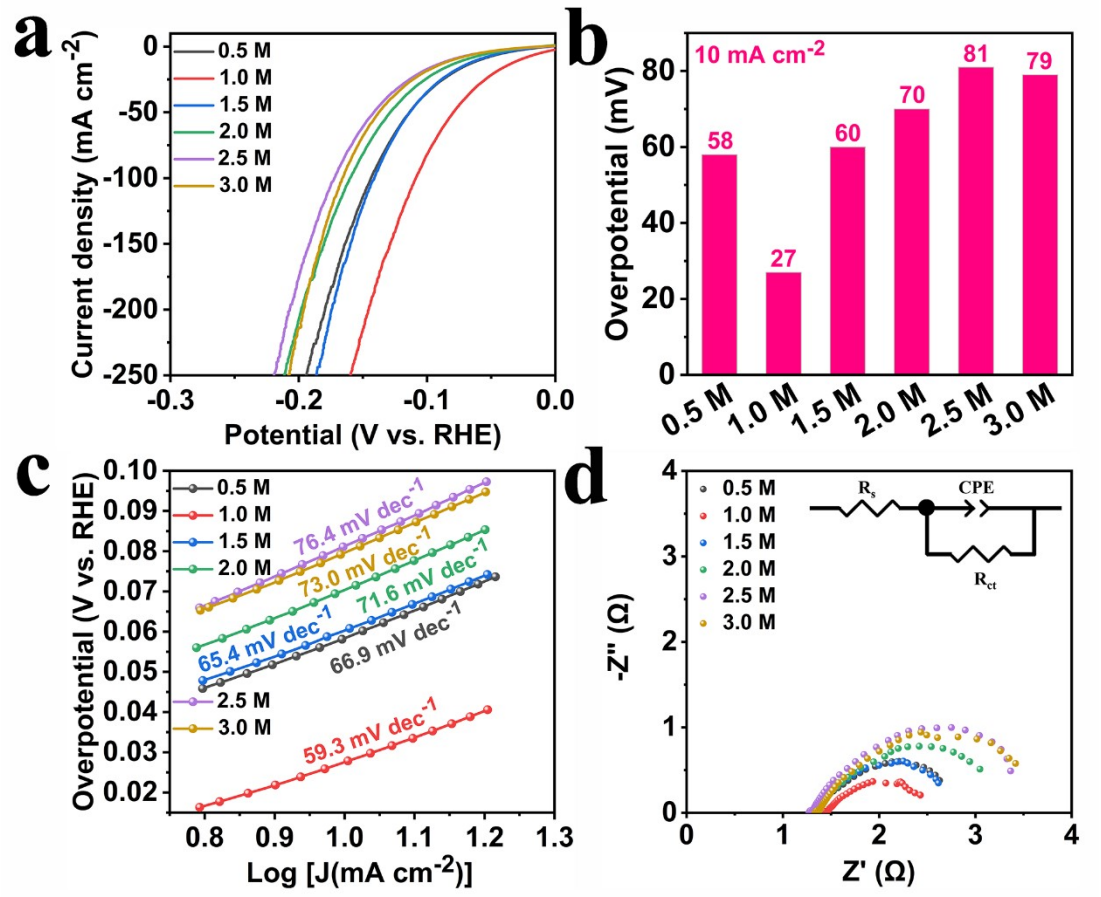

Fig. S21 The HER performance in 1.0 M KOH for FeOOH/S-Co catalysts prepared with different thiourea concentrations. (a) Polarization curves with a scan rate of 5 mV s^{-1}, (b) corresponding comparison of overpotentials at 10 mA cm^{-2}, (c) Tafel plots, (d) EIS curves.

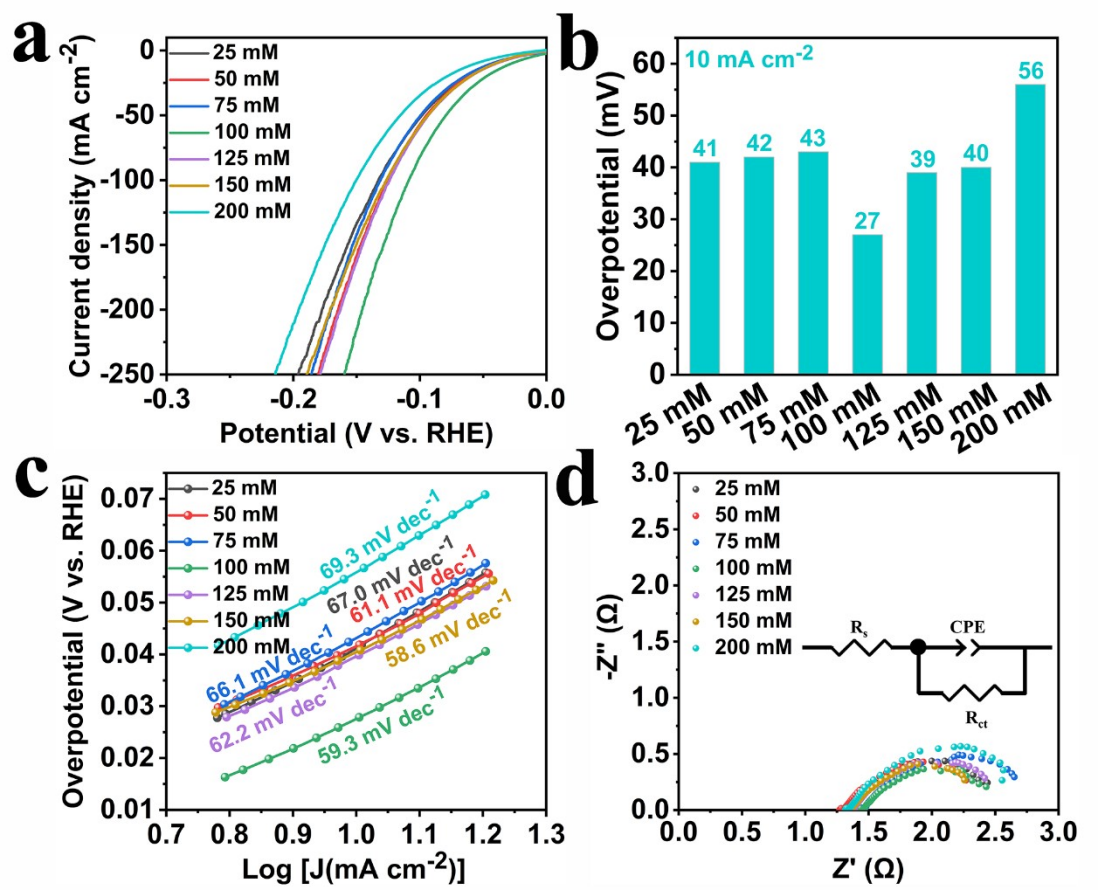

Fig. S22 The HER performance in 1.0 M KOH for FeOOH/S-Co catalysts prepared with different $FeSO_4$ concentrations. (a) Polarization curves with a scan rate of 5 mV s^{-1}, (b) corresponding comparison of overpotentials at 10 mA cm^{-2}, (c) Tafel plots, (d) EIS curves.

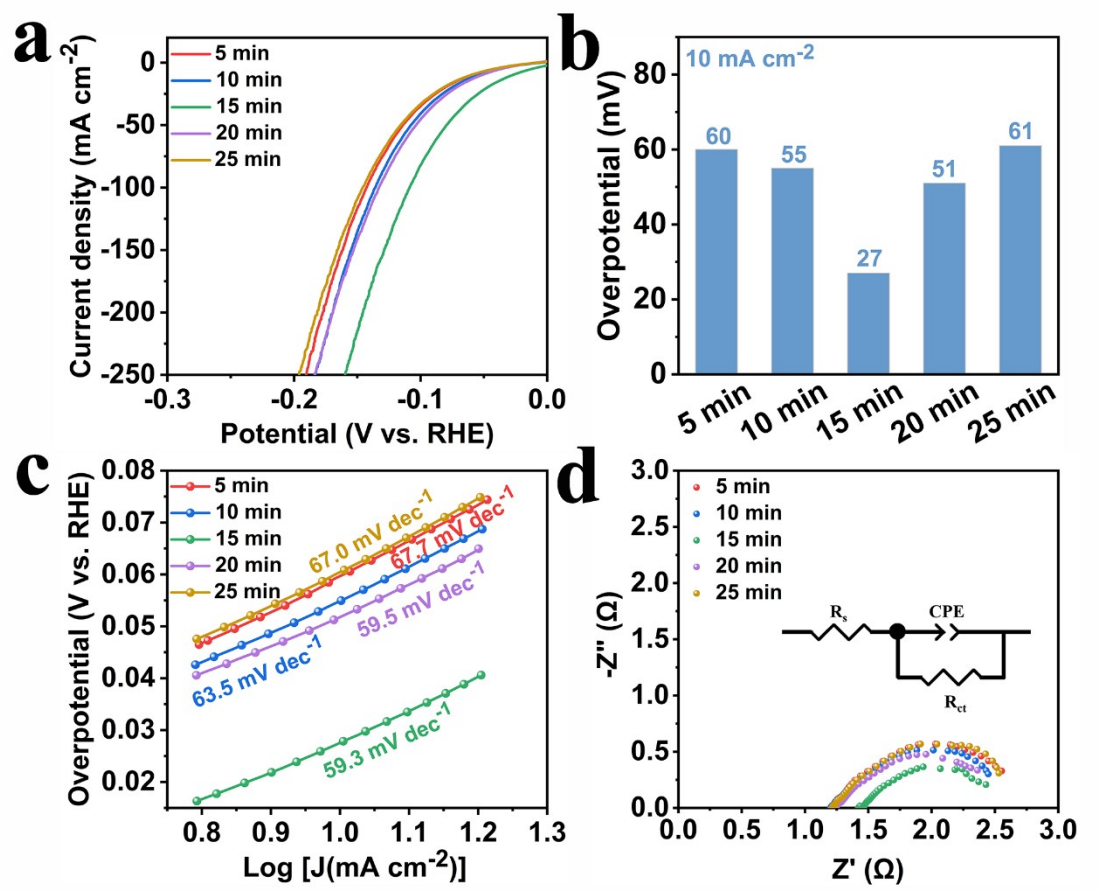

Fig. S23 The HER performance in 1.0 M KOH for FeOOH/S-Co catalysts prepared with different soaking time in $FeSO_4$. (a) Polarization curves with a scan rate of 5 mV s^{-1}, (b) corresponding comparison of overpotentials at 10 mA cm^{-2}, (c) Tafel plots, (d) EIS curves.

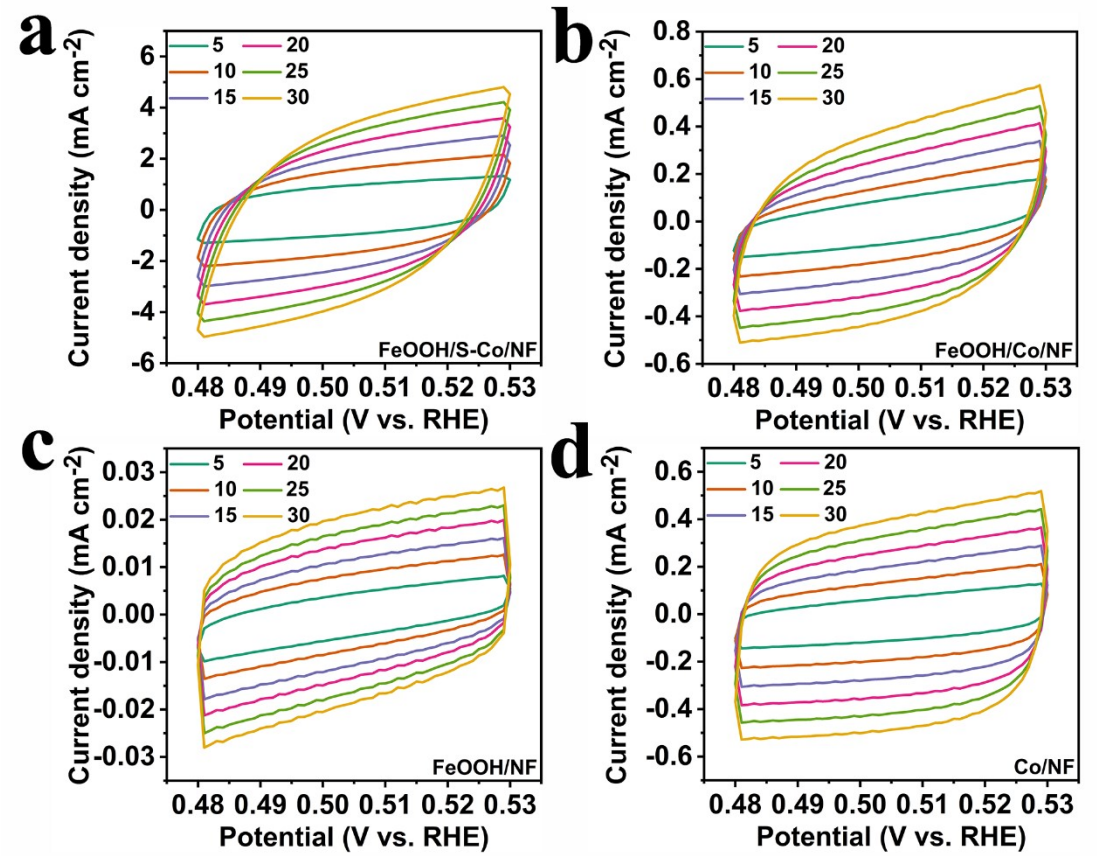

Fig. S24 CV curves of (a) FeOOH/S-Co/NF, (b) FeOOH/Co/NF, (c) FeOOH/NF and (d) Co/NF catalysts recorded in N_2-saturated 1.0 M KOH solution with different scan rates.

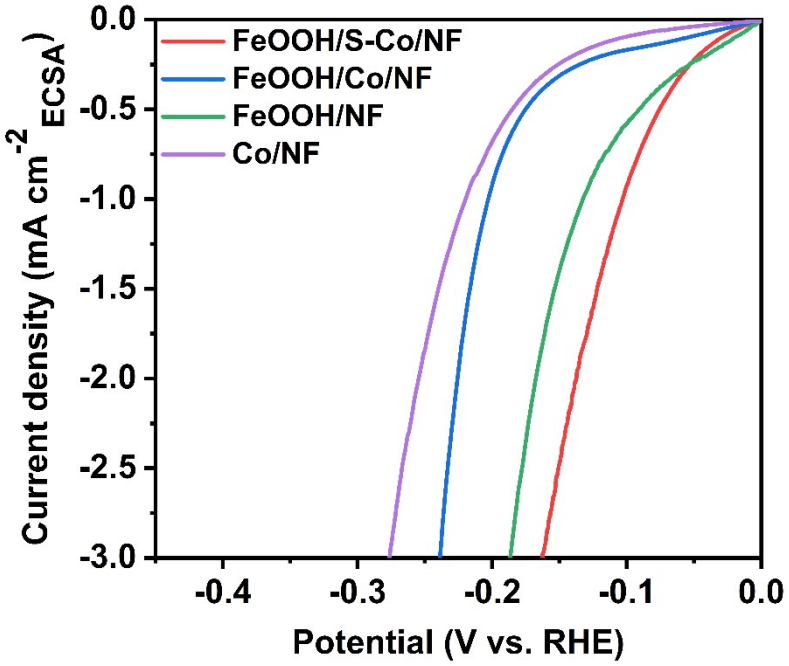

Fig. S25 The HER polarization curves normalized by ECSA for FeOOH/S-Co/NF, FeOOH/Co/NF, FeOOH/NF and Co/NF catalysts.

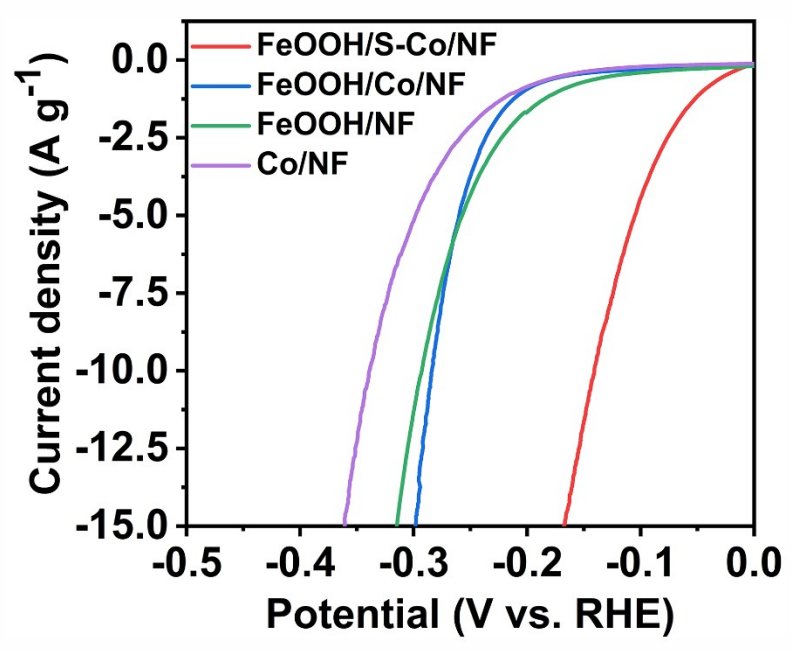

Fig. S26 The HER polarization curves normalized by mass for FeOOH/S-Co/NF, FeOOH/Co/NF, FeOOH/NF and Co/NF catalysts.

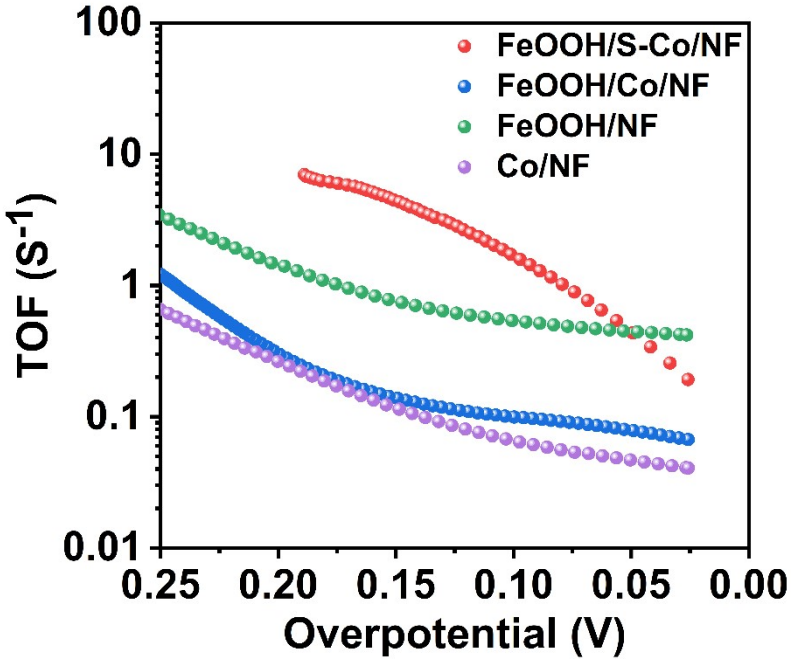

Fig. S27 The TOF values of FeOOH/S-Co/NF, FeOOH/Co/NF, FeOOH/NF and Co/NF catalysts for HER.

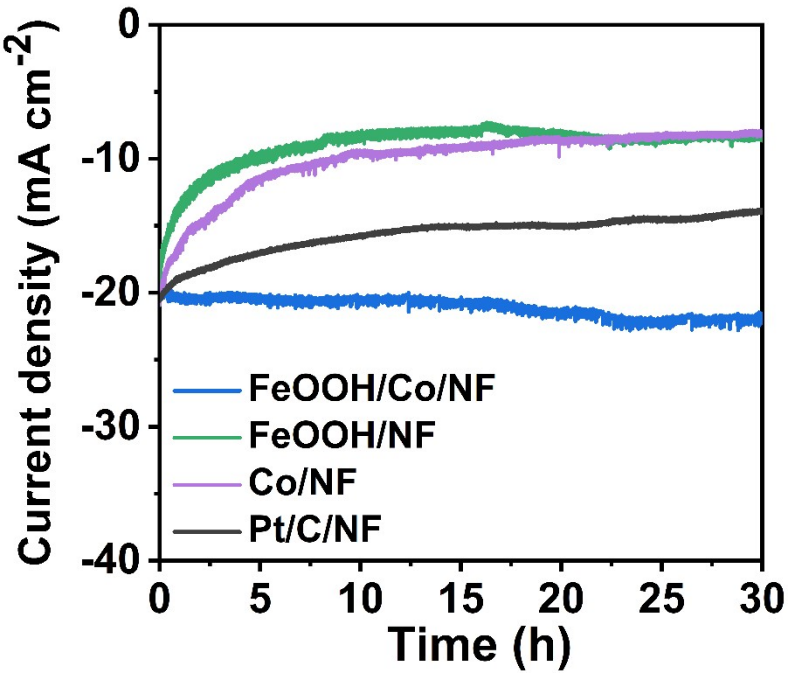

Fig. S28 I-t curves of FeOOH/Co/NF, FeOOH/NF, Co/NF and Pt/C/NF catalysts at −0.243 V, −0.298 V, −0.252V and −0.086 V for 30 h.

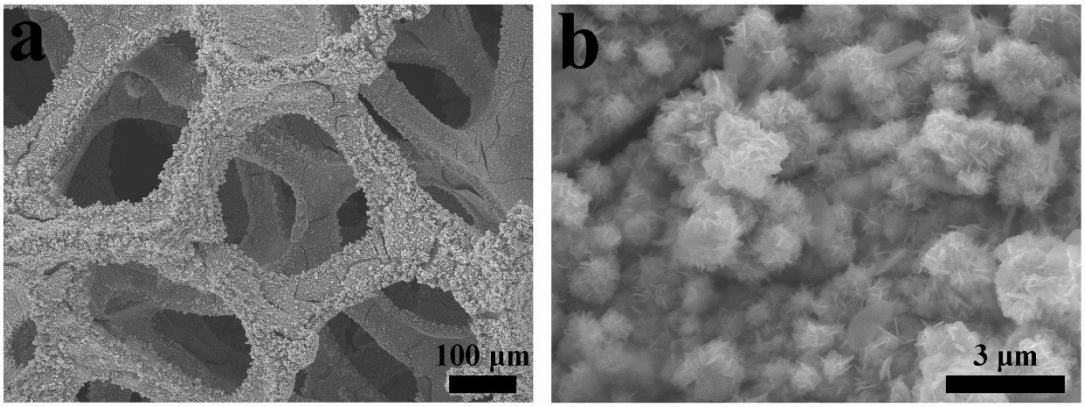

Fig. S29 The SEM images of FeOOH/S-Co/NF catalyst after HER i-t test at 20 mA cm^{-2} for 30 h.

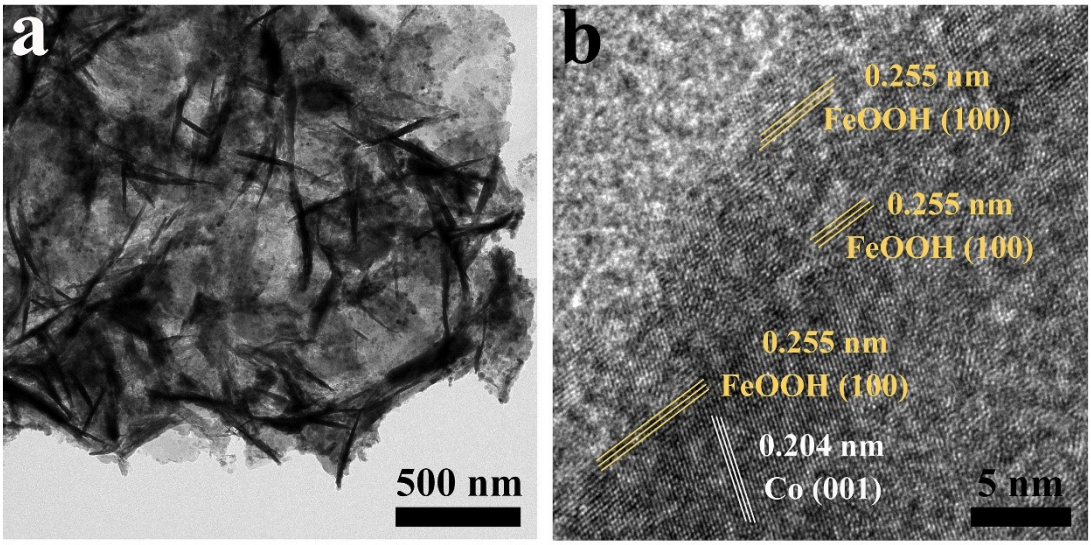

Fig. S30 (a) TEM and (b) HRTEM images of FeOOH/S-Co/NF catalyst after HER i-t test at 20 mA cm^{-2} for 30 h.

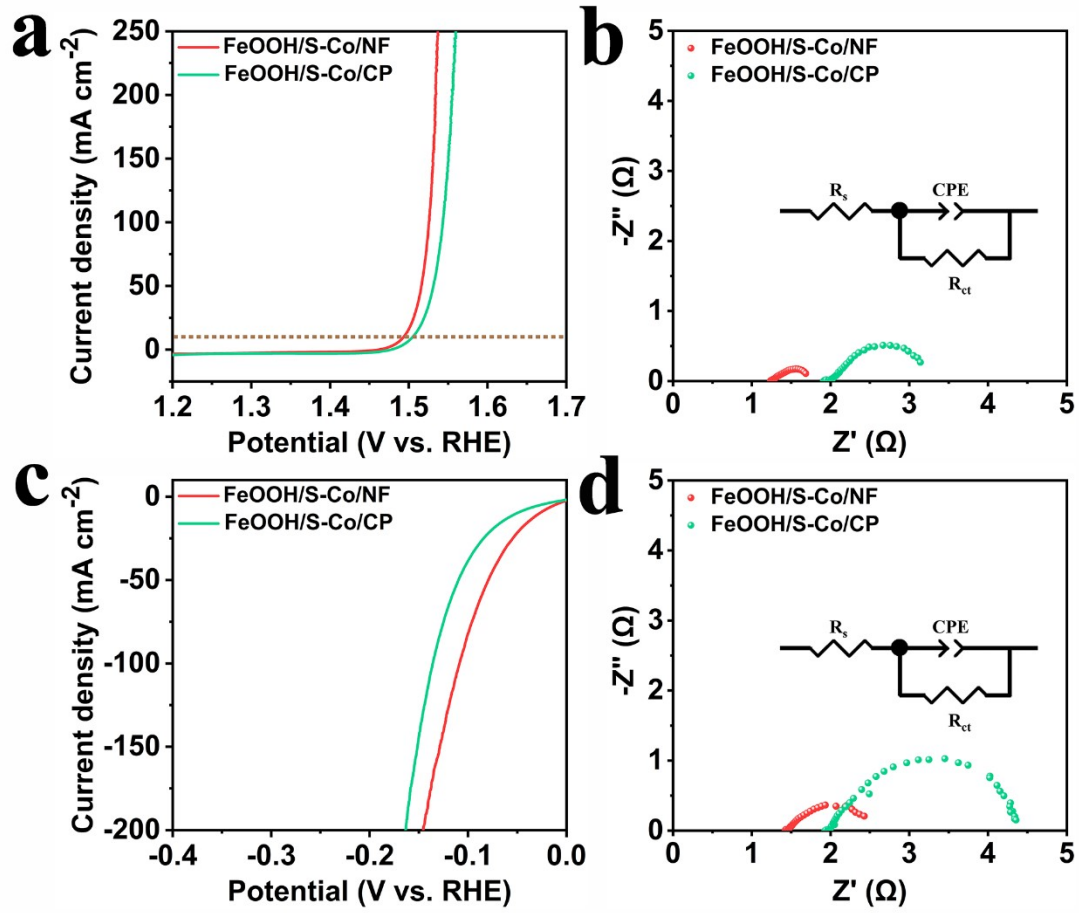

Fig. S31 (a) LSV curves and (b) EIS curves of FeOOH/S-Co/NF and FeOOH/S-Co/CP for OER. (c) LSV curves and (d) EIS curves of FeOOH/S-Co/NF and FeOOH/S-Co/CP for HER.

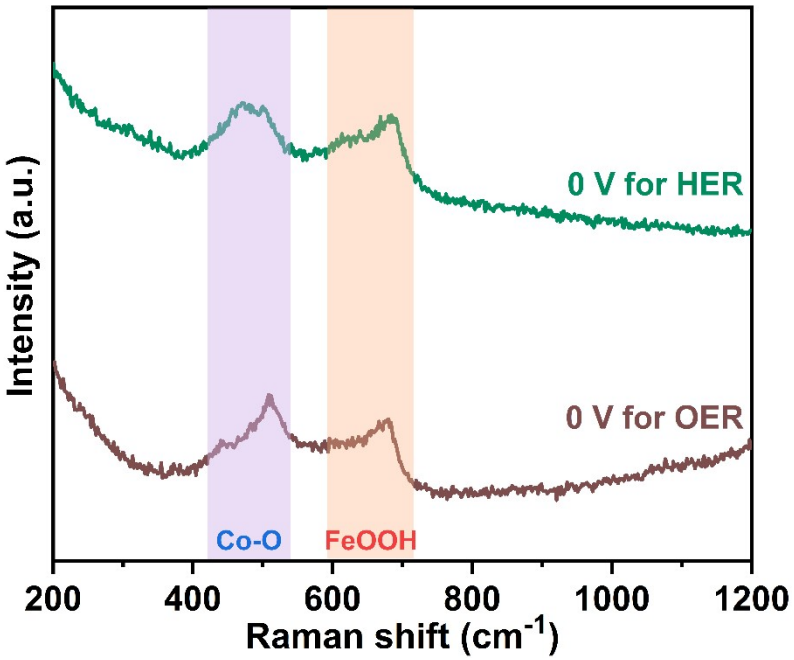

Fig. S32 In-situ Raman spectra of the FeOOH/S-Co/NF at 0 V for OER and HER in the same scale.

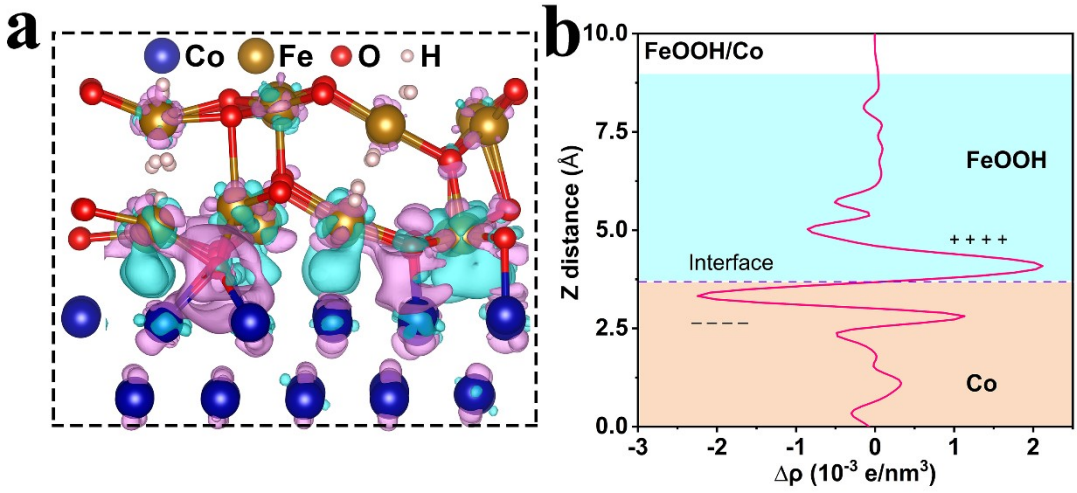

Fig. S33 (a) The differential charge density and (b) planar-averaged electron density difference of FeOOH/Co. The cyan region represents charge depletion and pink represents charge accumulation.

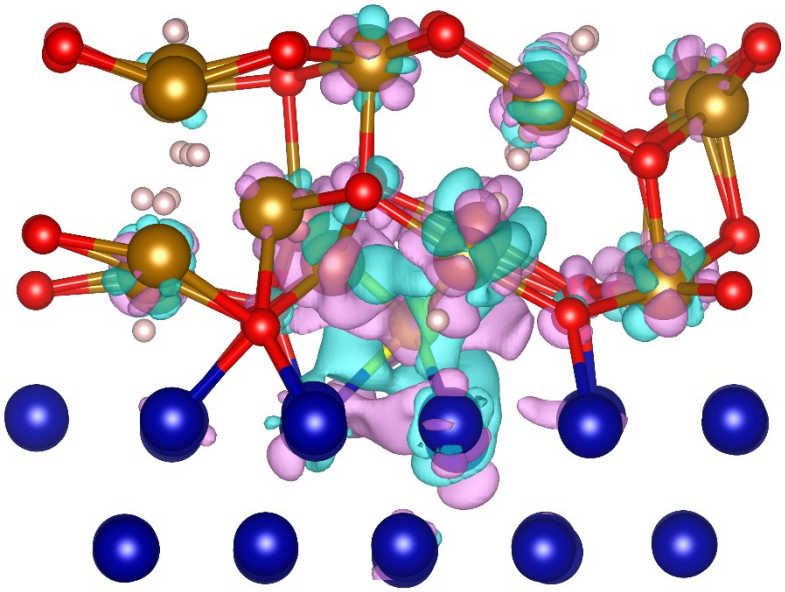

Fig. S34 Differential charge density of FeOOH/S-Co which is calculated through regarding Co and FeOOH as a whole. The cyan region represents charge depletion and pink represents charge accumulation.

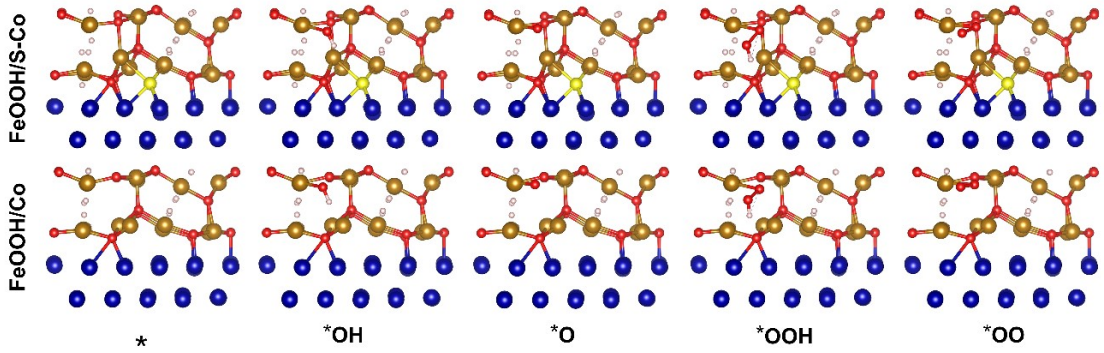

Fig. S35 Structures of the reaction intermediates through the OER process on FeOOH/S-Co (top) and FeOOH/Co (down) surfaces. Color code: blue, Co; brown, Fe; yellow, S; red, O; white, H.

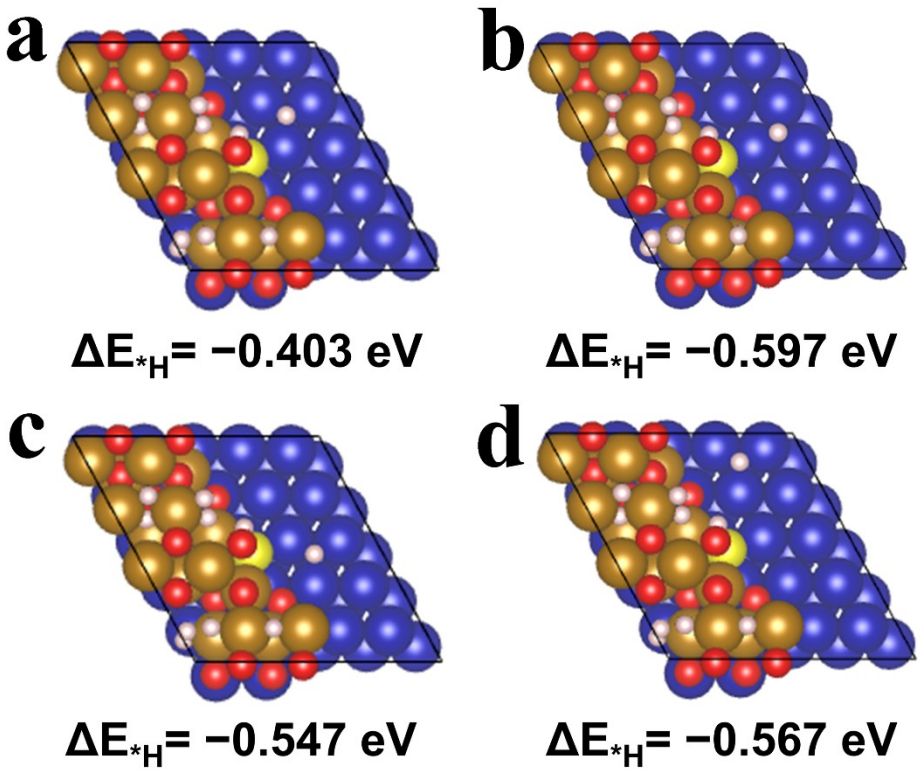

Fig. S36 Structures of the *H adsorption at different hollow sites of FeOOH/S-Co. Color code: blue, Co; brown, Fe; yellow, S; red, O; white, H.

Table S1. Elemental contents of different catalysts obtained from SEM-EDS measurement.

Catalysts	Co (At%/W%)	Fe (At%/W%)	S (At%/W%)	O (At%/W%)
FeOOH/S-Co/NF	46.74/68.85	7.99/11.15	4.71/3.77	40.56/16.22
FeOOH/Co/NF	76.20/88.71	4.78/5.28	/	19.02/6.01
FeOOH/NF	/	29.64/59.52	/	70.36/40.48
Co/NF	98.02/99.45	/	/	1.98/0.55
FeOOH/S-Co/NF after OER	49.65/70.96	7.98/10.81	4.57/3.56	37.79/14.66
FeOOH/S-Co/NF after HER	66.69/81.79	6.11/7.11	6.12/4.08	21.07/7.02

Table S2. EIS fitting results of FeOOH/S-Co/NF, FeOOH/Co/NF, FeOOH/NF, Co/NF, RuO_2/C/NF and NF catalysts for OER.

Catalysts	Solution series resistances R_s (Ω)	Charge transfer resistance R_{ct} (Ω)
FeOOH/S-Co/NF	1.25	0.58
FeOOH/Co/NF	1.30	0.76
FeOOH/NF	1.37	16.52
Co/NF	1.37	10.50
RuO_2/C/NF	1.43	4.19
NF	1.49	14.46

Table S3. Comparison of OER activity of FeOOH/S-Co/NF catalyst with reported Co/Fe-based electrocatalysts in 1.0 M KOH solution.

Catalysts	J (mA cm^{-2})	Overpotential (mV)	References
FeOOH/S-Co/NF	**10**	**264**	**This work**
	100	**294**	
Co/CoP@HOMC	10	260	Adv. Energy Mater. 2021, 2102134
P-Co_9S_8	10	280	Small 2019, 1904507
$NiCo_2O_4$	10	350	J. Mater. Chem. A 2020, 8, 17691-17705
$Co_{0.43}Ni_{0.57}$@C	10	296	Int. J. Hydrogen Energy 2022, 47, 3699-
CMN-500	10	290	Adv. Energy Mater. 2022, 12, 2103247
CoP/FeOOH	10	250	Chem. Eng. J. 2022, 428, 131130
Ni/Co_3O_4	10	311	Nano-Micro Lett. 2022, 14, 148
FeCoNC/SL	10	316	Adv. Sci. 2023, 10, 2205889
CoP/Co/C	10	320	J. Colloid Interface Sci. 2022, 623, 808-
Co-THB/CP	10	263	Small 2023, 2207720
Co/CoO@NC@CC	10	284	Chem. Eng. J. 2021, 414, 128804
NP Au/CoN_x	10	310	Adv. Mater. 2020, 32, 1907214.
S-FeOOH/IF	10	244	Adv. Funct. Mater. 2022, 32, 2112674
$CoSe_2$/ZnSe	10	320	ACS Nano 2019, 13, 5635-5645
Fe-NiO/NiS_2	10	270	Angew. Chem. Int. Ed. 2022,61,
FeOOH/Ni_3N	10	244	Appl. Catal., B 2020, 269, 118600
Mo-$NiCo_2O_4$/$Co_{5.47}N$	10	330	Small 2020, 16, 1906775

Table S4. Comparison of HER activity of FeOOH/S-Co/NF catalyst with reported Co/Fe-based electrocatalysts in 1.0 M KOH solution.

Catalysts	J (mA cm^{-2})	Overpotential (mV)	References
FeOOH/S-Co/NF	**10**	**27**	**This work**
	100	**100**	
Ni/FeOOH	10	38	Adv. Energy Mater. 2020, 10, 1904020
MoO_2/Co	10	48	J. Mater. Chem. A, 2022, 10, 17297-
Co-doped CeO_2	10	46	J. Am. Chem. Soc. 2020, 142, 6461-6466.
Co/MoN	10	52	Appl. Catal., B 2021, 286, 119882
$CoNiRuNT_3$	10	52	Adv. Mater. 2022, 34, 2107488
Pt@NiFe LDH	10	58	Small 2023, 2207044
FeP-CoP/NC	10	79	Nat. Commun. 2021, 12, 4143.
Co-NC-AF	10	85	Adv. Mater. 2021, 33, 2103533
FeP/Ni_2P	10	85	Nat. Commun. 2018, 9, 2551
Ni/Co_3O_4	10	93	Nano-Micro Lett. 2022, 14, 148
Co/Mo_2C@C	10	98	Chem. Eng. J. 2022, 430, 132697
δ-FeOOH/Ni_3S_2/NF	10	106	J. Mater. Chem. A 2020 , 8 21199
N-Co_9S_8/Ni_3S_2/NF	10	111	Small 2023, 2207425
Co/CoP@HOMC	10	120	Adv. Energy Mater. 2021, 2102134
CoP/Co/C	10	132	J. Colloid Interface Sci. 2022, 623, 808-
Co/CoO@NC@CC	10	152	Chem. Eng. J. 2021, 414, 128804
$Fe_{0.4}Co_{0.3}Ni_{0.3}$-1.8	10	175	Energy Environ. Mater. 2023, 0, e12590

Table S5. EIS fitting results of FeOOH/S-Co/NF, FeOOH/Co/NF, FeOOH/NF, Co/NF, Pt/C/NF and NF catalysts for HER.

Catalysts	Solution series resistances R_s (Ω)	Charge transfer resistance R_{ct} (Ω)
FeOOH/S-Co/NF	1.45	1.09
FeOOH/Co/NF	1.36	27.69
FeOOH/NF	1.36	109.00
Co/NF	1.33	35.33
Pt/C/NF	1.54	0.96
NF	1.42	64.71

Table S6. Comparison of water splitting performance of FeOOH/S-Co/NF catalyst with reported Co/Fe-based electrocatalysts in 1.0 M KOH solution.

Catalysts	J (mA cm^{-2})	Voltage (V)	References
FeOOH/S-Co/NF	**10**	**1.576**	**This work**
$Fe_{0.4}Co_{0.3}Ni_{0.3}$-1.8	10	1.62	Energy Environ. Mater. 2023, 0, e12590
Co/CoO@NC@CC	10	1.66	Chem. Eng. J. 2021, 414, 128804
Co/Mo_2C@C	10	1.59	Chem. Eng. J. 2022, 430, 132697
$Co_{0.43}Ni_{0.57}$@C	10	1.62	Int. J. Hydrogen Energy 2022, 47, 3699-3708
Ni/Co_3O_4	10	1.63	Nano-Micro Lett. 2022, 14, 148
Co_9S_8/Cu_2S/CF	10	1.60	ACS Appl. Mater. Interfaces 2021, 13, 9865-9874
FeOOH/Ni_3N	10	1.58	Appl. Catal., B 2020, 269, 118600
V-Ni_3S_2@NiFe LDH	10	1.55	J. Mater. Chem. A 2019, 7, 18118-18125
Co_3S_4@MoS_2	10	1.58	Nano Energy 2018, 47, 494-502
$Co(OH)_2$/Ag/FeP	10	1.56	ACS Appl. Mater. Interfaces 2019, 11, 7936-7945
d-Ni_3FeN/Ni_3Fe	10	1.61	J. Mater. Chem. A 2021, 9, 4036-4043

References

1. G. Kresse and J. Furthmuller, Efficient iterative schemes for ab initio total-energy calculations using a plane-wave basis set, *Phys. Rev. B*, 1996, **54**, 11169−11186.
2. G. Kresse and J. Furthmuller, Efficiency of ab-initio total energy calculations for metals and semiconductors using a plane-wave basis set, *Comput. Mater. Sci.*, 1996, **6**, 15−50.
3. P. E. Blöchl, Projector augmented-wave method, *Phys. Rev. B*, 1994, **50**, 17953−17979.
4. J. P. Perdew, K. Burke and M. Ernzerhof, Generalized gradient approximation made simple, *Phys. Rev. Lett.*, 1996, **77**, 3865−3868.